

Bond-Stretching-Phonon Anomalies in Stripe-Ordered $\text{La}_{1.69}\text{Sr}_{0.31}\text{NiO}_4$

J. M. Tranquada,¹ K. Nakajima,² M. Braden,^{3,4} L. Pintschovius,³ and R. J. McQueeney⁵

¹*Physics Department, Brookhaven National Laboratory, Upton, NY 11973, USA**

²*Neutron Scattering Laboratory, ISSP, University of Tokyo, Tokai, Ibaraki, Japan*

³*Forschungszentrum Karlsruhe, IFP, Postfach 3640, D-76021 Karlsruhe, Germany*

⁴*Laboratoire Léon Brillouin, CEA/CNRS, F-91191 Gif-sur-Yvette CEDEX, France*

⁵*Los Alamos National Laboratory, Los Alamos, NM 87545, USA*

(Dated: November 9, 2018)

We report a neutron scattering study of bond-stretching phonons in $\text{La}_{1.69}\text{Sr}_{0.31}\text{NiO}_4$, a doped antiferromagnet in which the added holes order in diagonal stripes at 45° to the Ni-O bonds. For the highest-energy longitudinal optical mode along the bonds, a softening of 20% is observed between the Brillouin zone center and zone boundary. At 45° to the bonds, a splitting of the same magnitude is found across much of the zone. Surprisingly, the charge-ordering wave vector plays no apparent role in the anomalous dispersions. The implications for related anomalies in the cuprates are discussed.

There is resurgent interest in the role of phonons with respect to the high-temperature superconductivity found in layered copper-oxides [1]. Particularly striking are the anomalies in high-energy optical modes observed by neutron scattering in $\text{La}_{2-x}\text{Sr}_x\text{CuO}_4$ [2, 3, 4] and $\text{YBa}_2\text{Cu}_3\text{O}_{6+x}$ [2, 5, 6, 7]. There have been various speculations as to whether the observed phonon anomalies might be related to instantaneous charge inhomogeneities, particularly those in the form of stripes [8]. Recently, detailed analyses of electron-phonon interactions in a dimerized stripe phase have been reported [9, 10].

One way to learn about the effect of charge stripes on lattice dynamics is to study a model system with well-defined stripe order. Here we present the first single-crystal study, to our knowledge, of the bond-stretching phonon modes in such a system, specifically $\text{La}_{2-x}\text{Sr}_x\text{NiO}_4$ with $x = 0.31$. The stripe order in Sr-doped nickelates has been characterized in detail by neutron diffraction, and the most recent summary of results is given in [11]. For $x \gtrsim 0.22$, the crystal structure is tetragonal, consisting of a body-centered stacking of NiO_2 planes. Within the NiO_2 planes, the charge stripes run diagonally along either [110] or $[\bar{1}\bar{1}0]$ directions, at 45° to the Ni-O nearest-neighbor bonds, which extend along [100] and [010] directions. (In contrast, the charge stripes observed in superconducting $\text{La}_{1.6-x}\text{Nd}_{0.4}\text{Sr}_x\text{CuO}_4$ run parallel to the Cu-O bonds [12]; however, for $x \lesssim 0.06$, the stripes inferred to exist in $\text{La}_{2-x}\text{Sr}_x\text{CuO}_4$ have the diagonal orientation of the nickelates [13, 14].) The maximum transition temperatures for charge-stripe and magnetic order occur at $x = \frac{1}{3}$ [11, 15]. Well below the charge-ordering temperature, T_{co} , the nickelates have very large resistivities [16, 17], consistent with all of the added holes being localized in charge stripes.

We focus on the highest-energy longitudinal optical modes propagating along the [100] and [110] directions. These modes show only weak dispersion in stoichiometric La_2NiO_4 [18]. In contrast, we observe a softening of 20% along [100] on moving from the Brillouin zone

center to the zone boundary, quite similar to that found in $\text{La}_{2-x}\text{Sr}_x\text{CuO}_4$ [3, 4]; along [110], a splitting of the same magnitude is observed over much of the zone and, in particular, at the zone boundary. These results are important for two reasons. 1) The observed anomalies must be associated with the local charge inhomogeneity. They are induced by the hole doping, and the holes are localized in the stripes. 2) There is no evidence that the charge-ordering wave vector, \mathbf{q}_{co} , plays a special role. If the phonon anomalies were related to collective phase fluctuations of the charge stripes, as in a conventional charge-density-wave system [19], then one might expect them to appear at \mathbf{q}_{co} . With the absence of a collective signature, it seems likely that the dominant effects involve local interactions between charge and lattice fluctuations.

Our $\text{La}_{2-x}\text{Sr}_x\text{NiO}_4$ crystal, grown by the floating-zone method, is cylindrical, with a diameter of 6 mm and length of 30 mm; the Sr concentration of $x = 0.31$ was confirmed by inductively-coupled plasma analysis (with an uncertainty of ± 0.01). At room temperature, the lattice parameters of the tetragonal unit cell are $a = 3.84 \text{ \AA}$ and $c = 12.70 \text{ \AA}$. The charge and spin ordering transitions were confirmed to be consistent with previous work [11] (magnetic and charge-order transitions of approximately 160 K and 235 K, respectively) by neutron diffraction measurements performed at the JRR-3M reactor in Tokai, Japan. The inelastic-neutron-scattering measurements of phonons were performed on the 1T triple-axis spectrometer at the Orphéé reactor of the Laboratoire Léon Brillouin in Saclay, France. The spectrometer is equipped with a Cu (111) monochromator and a pyrolytic graphite (PG) (002) analyzer, each of which is both vertically and horizontally focused. The analyzer was set to detect neutrons with a final frequency of 3.55 THz (14.7 meV). A PG filter was placed after the sample to minimize unwanted neutrons at harmonic wavelengths.

Figure 1(a) shows scans of scattered intensity versus excitation frequency for phonons propagating in the [100]

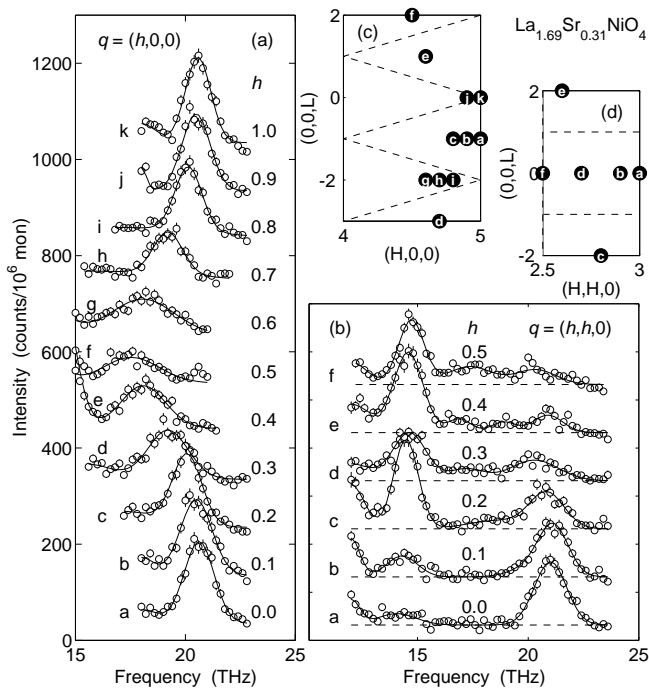


FIG. 1: Neutron scattering measurements of phonons in $\text{La}_{1.69}\text{Sr}_{0.31}\text{NiO}_4$ at $T = 10$ K. (a) Scattered intensity vs. frequency for reduced wave vectors, $\mathbf{q} = (h, 0, 0)$, varying from Brillouin zone center ($h = 0$) to the zone boundary ($h = 1$). Curves through the data are fits to gaussian peak shapes on top of a constant background. Scans have been offset vertically for clarity. (b) Similar results for $\mathbf{q} = (h, h, 0)$; dashed lines indicate the constant background. (c) and (d) indicate the positions in reciprocal space where the scans (identified by letters) of (a) and (b), respectively, were measured; dashed lines indicate Brillouin zone boundaries. Measurements were performed in various equivalent zones, with varying L -component, in order to avoid spurious peaks due to accidental Bragg scattering by the sample.

direction, parallel to the in-plane Ni-O bonds. The scans are taken at wave vectors along the line $\mathbf{q} = (h, 0, 0)$ in the first Brillouin zone, moving from the zone center ($h = 0$, bottom) to the zone boundary ($h = 1$, top), where the components of the wave vector are measured in reciprocal lattice units, $(2\pi/a, 2\pi/a, 2\pi/c)$. (The effective zone boundary for a single NiO_2 plane is at $h = 0.5$; the fact that the actual boundary is at $h = 1$ results from the body-centered stacking of the layers.) Each scan is dominated by a single, well-defined peak, that disperses from approximately 21 THz at zone center to less than 18 THz half-way across the zone, and then back up again. The lines through the data points are fitted gaussian peaks on top of a background that is taken to be independent of wave vector and frequency.

Figure 1(b) shows scans measured along the $[110]$ direction. Because of twinning of the stripe domains, we simultaneously probe phonons propagating parallel and

perpendicular to the stripes. Again, we focus on the mode that starts at about 21 THz at zone center; the mode at 14 THz involves bond-bending motion, and does not exhibit any notable doping-dependent behavior. [The intensity variation seen in the figure for this mode is associated with its sensitivity to the L -component of the wave vector \mathbf{Q} , which varies from point to point as noted in Fig. 1(d).] On moving from zone center to zone boundary, we note that the highest-frequency mode varies little in frequency, but it loses intensity. Concomitant with this, signal appears in the 17–18 THz regime, growing in strength as the zone boundary is approached.

Using the gaussian fits as a smoothed version of the data, we present our results as intensity plots in Fig. 2(a) and (b). Here, the intensity has been multiplied by ν/Q_{\parallel}^2 (Q_{\parallel} is the component of \mathbf{Q} along the phonon propagation direction) to correct for sensitivities of the neutron-scattering cross section. Dramatic differences are observed in the dispersions of the stripe-ordered system compared to those in stoichiometric La_2NiO_4 , which are indicated by the gray circles [18]. Contrary to naive expectations based on the Peierls-distortion model [19], there is no particular anomaly at the charge-ordering wave vector $\mathbf{q}_{\text{CO}} = (0.31, 0.31, 0)$ [see Fig. 2(b)]. Instead, we find a splitting of the mode along $[110]$ over a substantial part of the zone. The size of the dispersion in the $[100]$ direction is about the same as the $[110]$ splitting, and is essentially identical to the magnitude of the dopant-induced softening reported for superconducting $\text{La}_{1.85}\text{Sr}_{0.15}\text{CuO}_4$ [3, 4]. The softened modes are consistent with a previous study of the phonon density-of-states in $\text{La}_{2-x}\text{Sr}_x\text{NiO}_4$ [20], where a dopant-induced peak was observed at ~ 75 meV (≈ 18 THz).

Integrating the corrected intensity data of Fig. 2(a) and (b) over frequency yields the open circles shown in Fig. 2(c) and (d), respectively. The experimental results are compared with intensities calculated from the interatomic-potential model used to describe the phonons in $\text{La}_{1.9}\text{NiO}_{3.93}$ [18]. (An overall normalization of the calculated to the measured intensities has been applied in each panel.) The general consistency between the measured and calculated integrated intensities suggests that the distribution of weight for the anomalously-softened bond-stretching modes does not extend significantly below 16 THz.

To interpret our results, let us consider some simple phenomenological models. The high-energy bond-stretching phonons involve the motion of the in-plane oxygens between the much heavier nickel atoms. Suppose we assume the nickel atoms to be infinitely heavy and consider only nearest-neighbor forces; then each oxygen acts like an Einstein oscillator, with no dispersion of its vibrational frequency. Correcting for the finite mass of the nickel would result in a slight decrease in frequency towards the zone boundary; however, accounting for Coulomb repulsion between neighboring oxygen

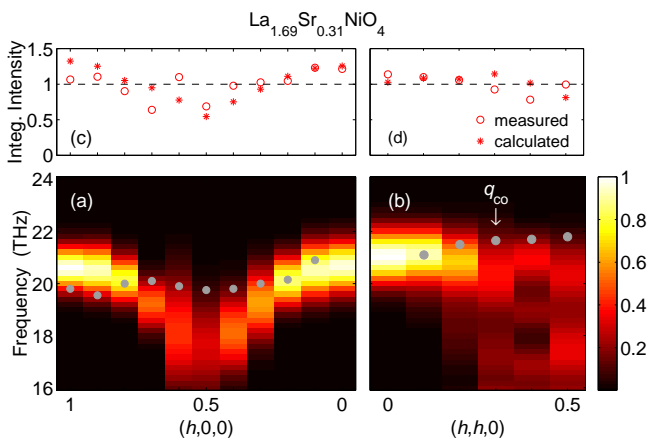


FIG. 2: (color) False-color images of intensity as a function of frequency and \mathbf{q} for (a) $\mathbf{q} = (h, 0, 0)$ and (b) $\mathbf{q} = (h, h, 0)$. The plotted intensity corresponds to the fitted curves (minus the background) from Fig. 2. q_{CO} indicates the approximate charge-ordering wave vector. The gray circles indicate the phonon dispersions measured in stoichiometric La_2NiO_4 [18]. (c) Intensity vs. \mathbf{q} integrated over frequency along the [100] direction. Open circles are data, stars are intensities calculated from the interatomic-potential model for $\text{La}_{1.9}\text{NiO}_{3.93}$ [18]. (d) Similar plot for the [110] direction.

ions would counter that with an increase in frequency at the zone boundary, where neighboring oxygens move opposite to one another. Ignoring these corrections, a simple Einstein model gives a rough approximation of the measured dispersions in stoichiometric La_2NiO_4 [18] [see Fig. 2(a) and (b)].

To go further, we will restrict ourselves to a linear Ni-O chain model. The softening of phonons at the zone boundary can be described by introducing a force between nearest-neighbor O ions with a negative force constant, k_{br} [18, 21] [see Fig. 3(a)]. This force phenomenologically incorporates a particular type of electron-phonon coupling. An example of the dispersion from such a model is shown in Fig. 3(c). The eigenvector for the softened zone-boundary mode, sketched in Fig. 3(e), involves linear breathing motion of the O about the Ni.

Next, suppose that k_{br} acts only between one pair of oxygens out of three [see Fig. 3(b)]. The result is a splitting of the modes, as illustrated in Fig. 3(d). Note that the intensity of the softened mode is strong at the zone boundary, but goes to zero at zone center. This effect is achieved without a dimerization of the lattice. As shown in Fig. 3(f), the eigenvector of the softened mode at zone boundary involves an isolated, local breathing motion of a pair of O about a Ni site. The behavior of this mode does not require coherence between motions in different unit cells.

It seems likely that both of these models have some degree of relevance to our observations; however, it is

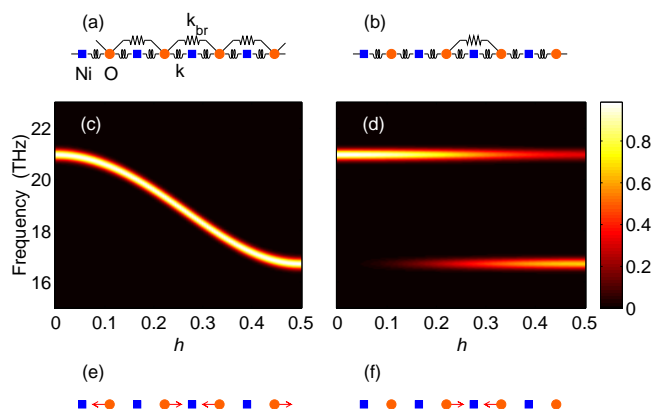


FIG. 3: (color) (a) Sketch of a force-constant model for a linear Ni-O array with a nearest-neighbor force constant of strength k , and an effective force constant k_{br} between next-nearest-neighbor oxygens. (b) Model with k_{br} acting only between one out of every three oxygen pairs. (c) Calculated intensity vs. $q = (2\pi/a)h$ and frequency for the model in (a) with $(2k/m_O)^{1/2}/2\pi = 21$ THz and $(-2k_{br}/m_O)^{1/2}/2\pi = 9$ THz. (d) Calculated intensity for model (b) with $(2k/m_O)^{1/2}/2\pi = 21$ THz and $(-k_{br}/m_O)^{1/2}/2\pi = 9$ THz. (e) Sketch of the eigenmode at $h = 0.5$ for model (a), corresponding to a linear breathing mode. (f) Softened eigenmode at $h = 0.5$ for model (b), corresponding to a local breathing mode.

difficult to associate them in a consistent or unique way with specific details of the measured dispersions. Of greater interest is the nature of the electron-phonon coupling modelled by k_{br} . In model calculations for $\text{La}_{2-x}\text{Sr}_x\text{CuO}_4$, Falter and Hoffmann [22] have emphasized the importance of ionic charge fluctuations in response to atomic displacements and the irrelevance of Fermi-surface nesting effects of the type once proposed by Weber [23]. Given the experimental evidence for poor electronic screening of phonons in optimally-doped cuprates [24], extended Coulomb interactions should also be important.

In the present case of the nickelate, little metallic screening is expected due to the gap of > 0.1 eV in the optical conductivity at low temperature [16, 25]. The bond-stretching modes involve polar fluctuations of the negative oxygen ions against the positive nickel ions, and so should couple to charge fluctuations. The lowest-energy channel for charge fluctuations must involve the dopant-induced holes, and since the holes are segregated into stripes, charge fluctuations must be associated with some form of stripe fluctuations.

In a conventional charge-density-wave (CDW) system, one might expect the mode along [110] to couple to fluctuations of the phase of the CDW with respect to the lattice [19]. In the present case, the absence of a characteristic wave vector suggests that local charge fluctuations may be more relevant for the bond-stretching modes. Lo-

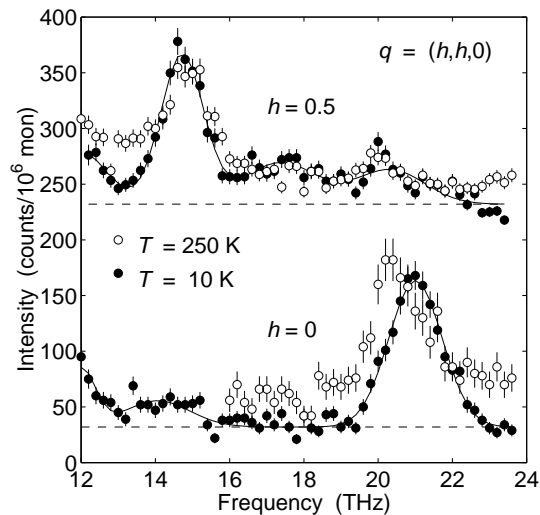


FIG. 4: Comparison of scans for $\mathbf{q} = (h, h, 0)$ at temperatures of 10 K (filled circles) and 250 K (open circles). The lines are the same as in Fig. 2. The upper scans have been shifted vertically by 200 counts.

cal fluctuations were predicted by Yi *et al.* [26] in a random-phase-approximation treatment of Hartree-Fock stripes. Nevertheless, our results do not rule out the possibility of weak, low-energy, collective phase fluctuations of the stripes.

Do the effects we observe depend on static ordering of the stripes? Figure 4 shows a comparison of phonons at zone-center and zone boundary along [110] measured at 10 K and 250 K, which is above the charge-ordering temperature. One can see that at 250 K, the zone-center mode has softened slightly but remains strong and well-defined; however, at the zone boundary, the intensity remains spread out in frequency. Thus, the anomalies do not disappear with the static order.

Rather similar phonon softenings were observed in the sample identified as $\text{La}_{1.9}\text{NiO}_{3.93}$ [18, 21]. Despite the specified stoichiometry, that sample exhibited superlattice peaks of the type $(H/2, K/2, L/2)$ with H , K , and L odd, consistent with the stage-2 ordering of interstitials found in $\text{La}_2\text{NiO}_{4.105}$ [27]. The latter compound exhibits evidence of incipient stripe correlations, but no stripe order [28]. This is further evidence that local interactions are sufficient to yield the phonon anomalies.

To summarize, we have observed doping-induced anomalies in bond-stretching modes of $\text{La}_{1.69}\text{Sr}_{0.31}\text{NiO}_4$, a compound in which the doped holes order in stripes at low temperature. The anomalies persist over a substantial portion of the Brillouin zone, with no obvious signature of collective stripe fluctuations. The splitting of the mode along [110] is similar to recent observations in superconducting $\text{Ba}_{0.6}\text{K}_{0.4}\text{BiO}_3$ [29], where charge inhomogeneity is also expected to be relevant. These results provide support for a connection between the phonon

anomalies observed in the cuprates and instantaneous charge inhomogeneity.

We gratefully acknowledge stimulating discussions with R. Werner and helpful comments from P. D. Johnson and S. A. Kivelson. This work was supported by the Materials Sciences Division, Office of Science, U.S. Department of Energy under Contract No. DE-AC02-98CH10886, and by the U.S.-Japan Cooperative Research Program on Neutron Scattering. JMT and KN wish to thank the staff of the Laboratoire Léon Brillouin for their hospitality during the experiments.

* Electronic address: jtran@bnl.gov

- [1] G.-M. Zhao, M. B. Hunt, H. Keller, and K. A. Müller, *Nature* **385**, 236 (1997); H. A. Mook and F. Doğan, *Nature* **401**, 145 (1999); A. Bussmann-Holder et al., *J. Phys.: Condens. Matter* **13**, L169 (2001); T. Schneider and H. Keller, *Phys. Rev. Lett.* **86**, 4899 (2001); A. Lanzara et al., *Nature* **412**, 510 (2001).
- [2] L. Pintschovius and W. Reichardt, in *Neutron Scattering in Layered Copper-Oxide Superconductors*, edited by A. Furrer (Kluwer, Dordrecht, The Netherlands, 1998), p. 165.
- [3] L. Pintschovius and M. Braden, *Phys. Rev. B* **60**, R15039 (1999).
- [4] R. J. McQueeney et al., *Phys. Rev. Lett.* **82**, 628 (1999).
- [5] W. Reichardt, *J. Low Temp. Physics* **105**, 807 (1996).
- [6] Y. Petrov et al., cond-mat/0003414.
- [7] R. J. McQueeney et al., cond-mat/0105593.
- [8] V. J. Emery, S. A. Kivelson, and J. M. Tranquada, *Proc. Natl. Acad. Sci. USA* **96**, 8814 (1999).
- [9] A.-H. Castro Neto, *Phys. Rev. B* **64**, 104509 (2001).
- [10] K. Park and S. Sachdev, *Phys. Rev. B* **64**, 184510 (2001).
- [11] H. Yoshizawa et al., *Phys. Rev. B* **61**, R854 (2000).
- [12] N. Ichikawa et al., *Phys. Rev. Lett.* **85**, 1738 (2000).
- [13] S. Wakimoto et al., *Phys. Rev. B* **60**, R769 (1999).
- [14] M. Fujita et al., cond-mat/0101320.
- [15] S.-W. Cheong et al., *Phys. Rev. B* **49**, 7088 (1994).
- [16] T. Katsufuji et al., *Phys. Rev. B* **54**, R14230 (1996).
- [17] T. Katsufuji et al., *Phys. Rev. B* **60**, R5097 (1999).
- [18] L. Pintschovius et al., *Phys. Rev. B* **64**, 094510 (2001).
- [19] H. J. Schulz, *Phys. Rev. B* **18**, 5756 (1978).
- [20] R. J. McQueeney, J. L. Sarrao, and R. Osborn, *Phys. Rev. B* **60**, 80 (1999).
- [21] L. Pintschovius et al., *Phys. Rev. B* **40**, 2229 (1989).
- [22] C. Falter and G. A. Hoffmann, *Phys. Rev. B* **64**, 054516 (2001).
- [23] W. Weber, *Phys. Rev. Lett.* **58**, 1371 (1987).
- [24] C. C. Homes et al., *Phys. Rev. Lett.* **84**, 5391 (2000).
- [25] Y. G. Pashkevich et al., *Phys. Rev. Lett.* **84**, 3919 (2000).
- [26] Y.-S. Yi, Z.-G. Yu, A. R. Bishop, and J. T. Gammel, *Phys. Rev. B* **58**, 503 (1998).
- [27] J. M. Tranquada et al., *Phys. Rev. B* **50**, 6340 (1994).
- [28] J. M. Tranquada, P. Wochner, and D. J. Buttrey, *Phys. Rev. Lett.* **79**, 2133 (1997).
- [29] M. Braden, W. Reichardt, S. Shiryayev, and S. N. Barilo, cond-mat/0107498.